

POLYESTER FABRICS COVERED WITH AMORPHOUS TITANIUM DIOXIDE LAYERS: COMBINING WETTABILITY MEASUREMENTS AND PHOTOINDUCED HYDROPHILICITY TO ASSESS THEIR SURFACE PROPERTIES

IRINA ZGURA, STEFAN FRUNZA, LIGIA FRUNZA*, MONICA ENCULESCU,
CAMELIA FLORICA, VALERIU FLORIN COTOROBAL, CONSTANTIN PAUL GANEA

National Institute of Materials Physics, PO Box Mg 07, 077125 Magurele, Romania

* E-mail: lfrunza@infim.ro

Received October 24, 2014

Abstract. Wettability properties of thin TiO₂ amorphous layers obtained by sputtering or sol-gel onto polyester textile materials were investigated. Contact angle (CA) measurements by the sessile drop method were used to evaluate these properties. Comparison was performed with coated samples of related poly(lactic acid) material. The samples coated by sol gel have CAs a few degrees higher than those coated by sputtering. Wetting properties were conversely changed under alternate darkness/illumination conditions. Photoinduced hydrophilicity was observed even for these amorphous coating particles, being higher for sputtered samples than for sol gel ones.

Key words: polyester fabrics, low temperature deposition, TiO₂ deposition, photo-induced hydrophilicity, wettability.

1. INTRODUCTION

Titanium dioxide TiO₂ (titania) is a transition metal oxide with very interesting UV absorbing properties leading to technological applications in many fields [1, 2]. In addition to applications of the bulk oxide, TiO₂ thin layers were obtained upon different materials for UV blocking, antibacterial or/and photo catalytic properties.

Coating the fibres by TiO₂ particles can be performed by several techniques [3–16]. Due to their low thermal stability, polyester (PES) fibres should be covered at rather low temperature [17–21], lower than that used for natural fibres. This fact limits the choice of deposition methods to be used in the case of polyester materials. We have covered thus some polyester fabrics [22] by two methods, sputtering or

sol-gel, both of them leading under temperature close to ambient conditions to amorphous layer of the oxide.

When covering the surface with (nano)particles a new roughness is added leading thus to a dual-size surface roughness. Therefore the study of wettability properties is a tool to test the surface functionalization. Moreover, it was indeed shown that TiO₂ particles induce photocatalytic properties [2] to the composite fabric-particle systems which are well correlated with the hydrophylicity of the covered textiles [23].

It is well known that wetting of a surface by a liquid is affected by the roughness of the surface [24]. In the case of textile materials, the roughness is related to the geometry which is very complex [25]. Due to the topography of the fibre, the construction of the yarn, and the construction of the fabric, polymer fibres, natural as well as synthetic might be made from porous materials and may take up water from the environment. Fabrics have thus pronounced texture, porosity, and also (oriented) in-plane capillarity along the threads. Contact angles on textile substrates can be useful quantities for comparative measurements in order to characterize the effects of surface modifications, especially if the textile is distinctly hydrophobic [25]. Thus CA measuring method was used in the aim of wettability search even in the case of complex materials as textiles (*e.g.* [26–29]).

This work intended to test the wettability properties of several polyester fabric samples covered with TiO₂ particles using sputtering or sol-gel methods. Due to the presence of carboxy groups, a sample of poly(lactic acid) (PLA) was also considered. Contact angle measurements were performed for quantitative evaluation of wettability. In addition, dynamically modifiable wettability by light irradiation was investigated as well: hydrophilicity appears on the film surface after UV irradiation as expected [23]. This is important especially because the layer proved to have photocatalytic properties in methylene blue decomposition [22].

We found that amorphous coated layers respond to illumination becoming hydrophilic, meaning that the investigated systems might be involved in photocatalytic applications.

2. EXPERIMENTAL

2.1. FABRIC SAMPLES

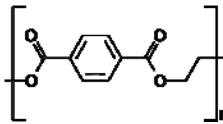
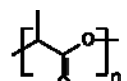
The investigated textiles were commercially purchased. Some properties are presented in Table 1.

Textile surface was modified by covering with TiO₂ using sputtering and sol-gel techniques; the deposition conditions were elsewhere detailed [22]. This surface modification was further called functionalization.

For comparison, glass plates (thoroughly pre cleaned) were deposited with TiO₂ at the same time with the textile samples.

Table 1

Textiles investigated for TiO₂ deposition

Sample label	Textile 2D-element/ thread*	Nature/formula of the fibres	Thickness [mm]	Density [g/cm ³]	Colour
PES2	Knitted/interlock/Nm	Polyester/ 	0.82	0.25	White
PES3	Knitted/interlock/Nm		0.89	0.26	White
PES28	Fabric warp Nm 70/2/ weft Nm 70/2		0.46	0.47	White
PES30	Fabric warp Nm 70/2/ weft Nm		0.52	0.41	White
PLA	Non-woven	Poly(lactic acid) / 	0.64	0.31	White

* Warp – the longitudinal threads; weft – the lateral threads. Nm means the length in meters per 1 g fabric mass.

Sample notation shows the treatment applied: the original (raw) samples have the material label of Table 1 for the ‘substrate’ while functionalized samples are noted TiO₂SPn/substrate or TiO₂SG/substrate where ‘substrate’ is the textile material. “n” is the pressure in the deposition chamber expressed as the number of 10² Pa; thus TiO₂SP8.6/PES2 means that the sputtering took place at a pressure of 8.6 × 10² Pa.

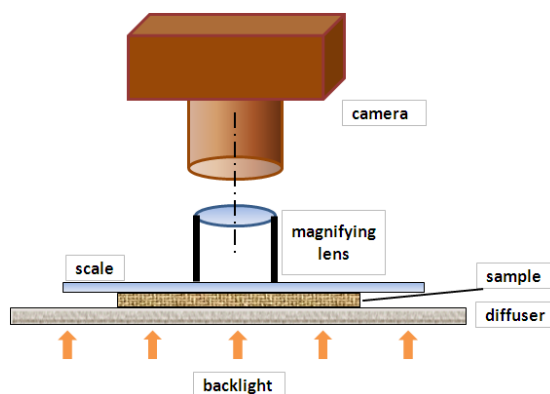


Fig. 1 – Experimental set-up for taking optical images: the light passes through a diffuser, the sample, the scale, a magnifying lens and enters the photo camera.

Both the original and the coated fabrics were complex characterized by applying the following techniques: X-ray diffraction (XRD) with a D8 Advance

equipment (Bruker-AXS), scanning electron microscopy (SEM) with a Zeiss Evo 50 XVP instrument, Fourier transform infrared spectroscopy (FTIR) with a Spectrum BX II (Perkin Elmer) spectrometer, thermal analysis (TA) with a Diamond TG-DTA apparatus (Perkin Elmer), optical microscopy performed with a set-up sketched in Fig. 1. Details on the measurements are given for similar systems in ref. [22, 29–31]. Optical images of the fabric samples were obtained in order to have a rapid comparison of the surface voids of the fabrics.

2.2. WETTING PROPERTIES

A highly polar liquid – water was recommended [32] as testing liquid in contact angle measurements, for estimating the wettability of polar solids as polyester materials. The water repellency was thus regarded as showing the performances of the coated layers and was evaluated by measuring static (equilibrium) contact angles at room temperature with Drop Shape Analyzer DSA 100 (Krüss). The working mode has been described elsewhere [31] for other types of materials. A fixed steel needle supplied a water drop of 3 μL onto the surface of the solid sample to be investigated. The image of the sessile (static) drops was captured; the data resulted from processing the images using specific programs to fit the profile with the Young-Laplace or polynomial of 2nd degree equations. Finally, one obtains the value of the equilibrium contact angles (CAs). At least five different points on each sample were thus considered.

2.3. UV-ILLUMINATION/DARKNESS EXPERIMENTS

Changes in the wetting properties were induced in the TiO_2 functionalized samples by exposure to illumination alternating with darkening conditions as follows: Irradiation with white light was performed for 210 min using an AM 1.5G solar simulator (Lot Oriel) with collimated output beam of 40 mm diameter, of min. 1 sun, an integrated electrical shutter with controller and a Xe lamp (300 W). The sample was positioned at 10 cm to the source. UV irradiation was performed with different illumination times with a LS150-Xe free ozone lamp (Lot Oriel) in a geometry allowing a short distance (of 30 cm) to the tissue. Darkening conditions were ensured in a specially designed black box.

3. RESULTS AND DISCUSSION

X-ray diffraction and scanning electron microscopy indicate that TiO_2 coating particles are amorphous. Sputtered layers consist in aggregates randomly distributed on the substrate while the sol gel layers show a uniform coverage of nanoparticles having a mosaic-like structure. The loading degree is ca. 2%. The

coated samples present photocatalytic activity in the methylene blue degradation [22]. Here we give and discuss the wettability properties: firstly, the effect of the functionalization with TiO₂ nanoparticles on the contact angle values; then the changes in the wettability induced by the sample exposure to the UV-illumination/darkness.

3.1. WETTABILITY PROPERTIES

Representative images of the water droplets onto the coated PES2 samples leading to the evaluation of the contact angle are given in Fig. 2. The measurements were performed for a direction parallel to the direction of vertical advance of the knitted matter because there are differences of a few degrees when the measurements are performed following a direction parallel against the perpendicular direction.

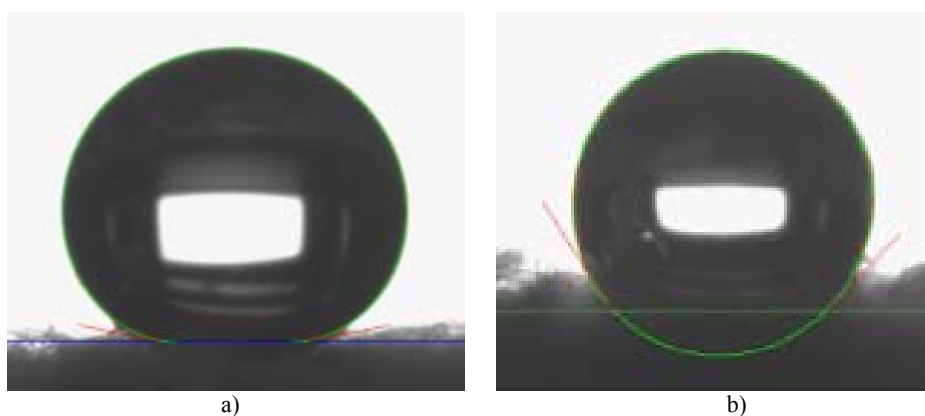


Fig. 2 – Water droplets in contact with the surface of: a) TiO₂SG/PES2 (169.3/169.3); b) TiO₂SP8.6/PES2 (133.2/134.4) samples. Values of the left/right CAs are given in parentheses. The shape contour and the left/right tangents are drawn as well. Small fibres can be observed on the material surface.

The surfaces investigated are far from being flat, smooth and homogeneous: Textile surfaces are rough and the experimentally measured contact angle is in fact an apparent one; it can differ considerably from the true value. The mean CA values of the raw or coated samples are given in Table 2.

All the raw materials are hydrophobic, with CA > 90°. When comparing these values with the CA (of 84°) of extruded polymer films cleaned thoroughly [33], one can say that the fabrics have larger contact angles. CAs increase more by fabric modification (titania deposition). CAs were formed among air, water droplet and the surface of fabric, in the presence of nanoroughness as it was recently suggested [27]. Some samples having CA > 150°, can be considered super-

hydrophobic. One sample (P28) is hydrophilic meaning that water passes through it; this sample has voids enough large (Fig. 3) and the margins become hydrophilic by deposition of hydrophilic particles. On the PLA sample the water droplet was sitting on the felt part of the material (black parts in Fig. 3c). These CA measurements can be then used for a primary evaluation of the coating morphology.

Table 2

Contact angle values of water onto the surface of investigated samples

Sample	CA /degree	$f = \frac{1 + \cos \theta_c}{1 + \cos \theta_0} *$
PES2	136.9	0.24457
PES3	138.1	0.23188
PES28	152.1	0.10598
PES30	124.8	0.38949
PLA	129.6	0.3288
TiO ₂ SG/PES2	169.3	0.01782
TiO ₂ SG/PES3	169.7	0.01683
TiO ₂ SG/PES28	152.7	0.11089
TiO ₂ SG/PES30	158.9	0.06733
TiO ₂ SG/PLA	140.6	0.22574
TiO ₂ SP4/PES2	133.8	0.20981
TiO ₂ SP4/PES3	166.0	0.02044
TiO ₂ SP4/PES28	Hydrophylic	0.6812
TiO ₂ SP4/PES30	155.8	0.05995
TiO ₂ SP4/PLA	150.3	0.08992

* θ_0 was taken as 84° for the raw samples, 89.4° for the sol-gel coated samples and 62.1° for the sputtered ones.

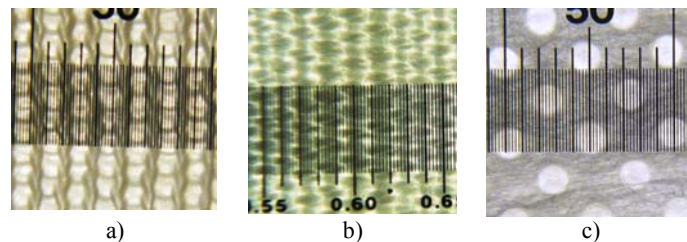


Fig. 3 – Optical images at the same magnitude (shown by the scale) of some textile materials in original form: a) PES2; b) PES28; c) PLA.

In addition to the roughness increase by deposition, when more air is trapped in-between the structures, the voids (pores) are smaller for deposited samples than for original samples, a fact which tends to slow down the diffusion. The phenomena are complex and it is rather difficult to separate them.

TiO₂ particles seem uniformly distributed on the fabric surface [22] but it is more reasonable to consider that they grow on scattered places and do not cover the surface completely; inside the fabric the fibres surfaces are also covered by TiO₂ particles. Higher CA might be due to the droplet on the surface of a composite surface, formed among air, water droplet and the fabric, in presence of nanoroughness as it was suggested recently by [34]. The behaviour might be approximated by the Cassie-Baxter equation in the form:

$$\cos \theta_c = f \cos \theta_0 - (1 - f),$$

where θ_c is the composite contact angle formed on the treated fabric and θ_0 is the contact angle formed on untreated fabric [27]. The f parameter is the fraction of the surface contacting the water droplet. The values of f can be calculated for each pair raw-treated samples as $f = (1 + \cos \theta_c) / (1 + \cos \theta_0)$ by knowing the corresponding CAs. These values are given also in Table 2: they are positive but some of them, rather low (a few hundredths). However, it seems that Cassie-Baxter equation (or Wenzel equation) should be applied to superhydrophobic surfaces with caution [35]. TiO₂ can be utilized to lead hydrophobic surfaces by creating artificial roughness via microstructuring [36].

Although bulk polyester is hydrophobic, the textile contact with water droplets shows the disappearance of water droplets due to high porosity (void areas) of the material allowing for water penetration through the microstructure. The void areas are reduced by the addition of TiO₂. These particles decrease the voids and concomitantly increase the sample hydrophobicity. Under these complex conditions one cannot use the traditional equations like Cassie-Baxter or Wenzel (see a recent review [37]) to model the wettability behaviour of the heterogeneous and rough samples.

The contact angles obtained by us onto coated glass plates have the values of 89.4° onto the sol-gel coated sample and 62.1° onto the sputtered (at the highest deposition pressure) one, in good agreement to those found in the literature for an amorphous layer [38] namely of 34° and 66° for the as-coated thin films on a flat substrate through the peroxotitanate-complex or the liquid-phase deposition methods, respectively, which slowly increased to about 70° and 73° after being stored in air. These values were used in calculations of f parameter in Table 2.

3.2. PHOTOINDUCED (SUPER)HYDROPHILICITY BY EXPOSURE TO THE UV-ILLUMINATION / DARKNESS

Photoinduced superhydrophilicity is now a notorious effect observed for the films or crystals of TiO₂ (see a review in ref. [39] or the references cited in a recent work [40]). As a result of illumination, contact angles of even (close to) 0° (hydrophilicity) were reported for water. It was also reported that the light induced

hydrophilic surface can be reversed to a hydrophobic one when the TiO₂ bearing system was kept in the dark for a period of time. Table 3 collects some of our results for the induced hydrophilicity.

Table 3

Values of the contact angle CA_{irr} of water onto coated samples after irradiation for 210 min

Sample	CA _{irr} /degree
TiO ₂ SG/PES2	154.8
TiO ₂ SG/PLA	143.0
TiO ₂ SP4/PES2	Hydrophilic
TiO ₂ SP4/PLA	117.7
TiO ₂ SP8.6/PES2	Hydrophilic
TiO ₂ SP8.6/PLA	Hydrophilic
TiO ₂ SP40/PES2	155.7
TiO ₂ SP40/PLA	31.1

It is found that TiO₂ films prepared by the sol–gel method exhibited lower hydrophilicity after illumination, compared to TiO₂ films prepared by sputtering. From Table 3 we see also that CA decreases to complete hydrophilicity by illumination for TiO₂SP4/PES2 sample but increases (with ca. 18⁰) for the sample TiO₂SP40/PES2. Lee *et al.* arrived at similar conclusions [41]. Furthermore, the hydrophilicity can be explained by using the theory according to which a layer of adsorbed hydroxyl (OH) and multiple layers of water molecules [42] exist; it seemed that the hydrophilic property was mostly determined by change of surface state within a few topmost layers of films.

The sensibility of the layers coated by sputtering to the UV illumination higher than those coated by sol-gel resulted from the experiments as function of the illumination time as well. These experiments can be illustrated as in Fig. 4, in which hydrophilicity of the samples was evaluated as the decrease (in percent) of the contact angle value. The behaviour of our samples is similar with that found in the literature for the variation of the contact angle with irradiation time [40].

We mention that 16 h under the darkness is enough to restore the hydrophobic properties for all these samples.

Hydrophilicity of amorphous TiO₂ layer has been reported [38] to be ascribed to the chemisorption of the water molecules to the Ti³⁺ sites generated by photoreduction of surface Ti⁴⁺, which in turn is closely related to the oxygen

bridging sites. We have no argument in this sense but it is quite plausibly that our samples behave in a similar mode.

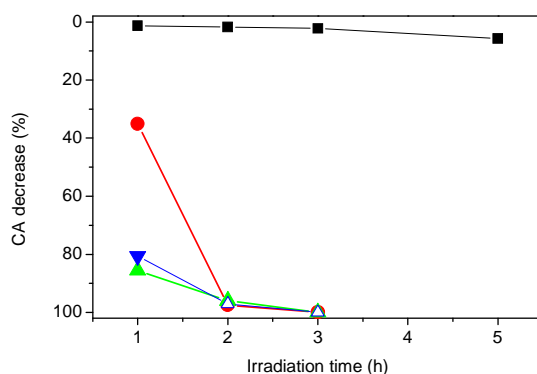


Fig. 4 – Decrease of the contact angle vs. time of UV irradiation for the following samples: TiO₂SG/PES2 (squares); TiO₂SP8.6/PES2 (circles); TiO₂SG/PLA (up triangles); TiO₂SP8.6/PLA (down triangles). Lines are guide for eyes. The errors are $\pm 4.2\%$.

The low temperature deposition process was thus successful for the polyester fabrics which are a less active material. The composite materials present photoactivity in a test reaction and also photoinduced hydrophylicity as sign of photoinduced catalytic activity. However, for applications, the best deposition parameters and the reactions conditions have to be established.

4. CONCLUSIONS

Polyester and poly(lactic acid) textile samples coated with TiO₂ particles at low temperature using either a sputtering or a sol gel technique were structurally and morphologically characterized:

Wetting properties evaluated by contact angle measurements have shown that the raw materials are hydrophobic, with CA higher than 90°. CA mostly increases with a few degrees in the case of PES samples and up to 20° for PLA by the TiO₂ deposition. The samples coated by sol gel have a few degrees higher CA than those coated by sputtering. In addition, there is a photoinduced superhydrophilicity for the coated samples, despite the deposition method, but the layer prepared by the sol–gel exhibited lower hydrophilicity after illumination, compared to TiO₂ films prepared by sputtering. The influence of argon pressure in the deposition chamber is quite effective since CA increases (with ca. 18°) by deposition at 4×10^3 Pa against that coated at 4×10^2 Pa.

The sensitivity of the layers coated by sputtering to the UV illumination higher than for those coated by sol-gel clearly resulted from the irradiation experiments as function of the time. This might indicate that the nanoparticle agglomerates randomly distributed on the substrate interact easier with the photons than the uniform mosaic-like structure coated by sol-gel.

Acknowledgements. The authors gratefully thank the Romanian Authority of the Education Ministry for the financial support under the project ID 281/2011, Dr. A. Dorogan (National Institute for Textile & Leather, Bucharest) for some textile samples, Dr. G. Socol (National Institute for Lasers, Magurele) for the illumination/darkening experiments.

REFERENCES

1. O. Carp, C.L. Huisman, A. Reller, *Progr. Solid State Chem.* **32**, 33–177 (2004).
2. K. Hashimoto, H. Irie, A. Fujishima, *Jap. J. Appl. Phys.* **44**, 8269–8285 (2005).
3. J.O. Carneiro, V. Teixeira, J.H.O. Nascimento, J. Neves, P.B. Tavares, *J. Nanosci. Nanotechnol.* **11**, 8979–8985 (2011).
4. A. Singh, E.A. Davis, *J. Non-Cryst. Solids* **122**, 223–232 (1990).
5. Y. Xu, W. Xu, F. Huang, *J. Eng. Fibers Fabrics* **7/4**, 7–12 (2012).
6. Y. Xu, W. Xu, F. Huang, Q.F. Wei, *Int. J. Photoen.* 852675 (2012).
7. A. S. da Silva Sobrinho, G. Czeremuskin, M. Latreche, M.R. Wertheimer, *J. Vac. Sci. Technol. A* **18**, 149–157 (2000).
8. J. Madocks, J. Rewhinkle, L. Barton, *Mater. Sci. Eng. B* **119**, 268–273 (2005).
9. Y. Leterrier, *Progr. Mater. Sci.* **48**, 1–55 (2003).
10. A. Sonnenfeld, R. Hauert, P. R. von Rohr, *Plasma Chem. Plasma Proc.* **26**, 319–334 (2006).
11. M. Asadi, M. Montazer, *J. Inorg. Organomet. Polym. Mater.* **23**, 1358–1367 (2013).
12. A. Ojstrsek, K. S. Kleinschek, D. Fakin, *Surf. & Coatings Technol.* **226**, 68–74 (2013).
13. M. Rehan, A. Hartwig, M. Ott, L. Gätjen, R. Wilken, *Surf. & Coatings Technol.* **219**, 50–58 (2013).
14. L. Surdu, M.D. Stelescu, E. Manaila, G. Nicula, O. Iordache, L.C. Dinca, M.-D. Berechet, M. Vamesu, D. Gurau, *Bioinorg. Chem. Appl.* **2014**, 763269 (2014).
15. P. Pisitsak, A. Samootsoot, N. Chokpanich, *KKU Res. J.* **18**, 200–211 (2013).
16. Y. Watanabe, T. Kobayashi, S. Kirihara, Y. Miyamoto, K. Sakoda, *Eur. Phys. J. B* **39**, 295–300 (2004).
17. I. Karbownik, D. Kowalczyk, G. Malinowska, B. Paruch, *Acta Phys. Pol. A* **116**, S-169-S-171 (2009).
18. I.A. Tudor, M. Petriceanu, R.-R. Piticescu, R.M. Piticescu, C. Predescu, *U.P.B. Sci. Bull., Ser.B.* **76**, 207–215 (2014).
19. H. Li, H. Deng, J. Zhao, *Intern. J. Chem.* **1**, 57–62 (2009).
20. H.S. Jung, H. Shin, J.R. Kim, J.Y. Kim, K.S. Hong, *Langmuir* **20**, 11732–11737 (2004).
21. W.A. Daoud, J.H. Xin, Y.-H. Zhang, K. Qi, *J. Non-Cryst. Solids* **351**, 1486–1490 (2005).
22. I. Zgura, S. Frunza, L. Frunza, M. Enculescu, C. Florica, C.P. Ganea, C.C. Negrila, L. Diamandescu, *J. Optoelectr. Adv. Mater.*, submitted 2014.
23. V.V. Vinogradov, A.V. Agafonov, A.V. Vinogradov, *Mendeleev Comm.* **23**, 286–288 (2013).
24. J.D. Miller, S. Veeramasuneni, J. Drelich, M.R. Yalamanchili, G. Yamauchi, *Polymer Eng. Sci.* **36**, 1849–1855 (1996).
25. T. Bahners, *J. Adhesion Sci. Technol.* **25**, 2005–2021 (2011).
26. G. Qia, H. Zhang, Z. Yuan, *Appl. Surface Sci.* **258**, 662–667 (2011).

27. M. Ashraf, C. Campagne, A. Perwuelz, P. Champagne, A. Leriche, C. Courtois, *J. Colloid Interface Sci.* **394**, 545–553 (2013).
28. G.Y. Bae, B.G. Min, Y.G. Jeong, S.C. Lee, J.H. Jang, G.H. Koo, *J. Colloid Interface Sci.* **337**, 170–175 (2009).
29. A. C. Popescu, L. Duta, G. Dorcioman, I. N. Mihailescu, G. E. Stan, I. Pasuk, I. Zgura, T. Beica, I. Enculescu, A. Ianculescu, I. Dumitrescu, *J. Appl. Phys.* **110**, 064321 (2011).
30. L. Frunza, N. Preda, E. Matei, S. Frunza, C. P. Ganea, A. M. Vlaicu, L. Diamandescu, A. Dorogan, *J. Polym. Sci. Polym. Phys.* **51**, 1237–1247 (2013).
31. I. Zgura, T. Beica, I. L. Mitrofan, C. G. Mateias, D. Pirvu, I. Patrascu, *Dig. J. Nanomater. Bios.* **5**, 749–755 (2010).
32. M. Voinea, C. Vladuta, C. Bogatu, A. Duta, *Mater. Sci. Eng. B* **152**, 76–80 (2008).
33. E. Bormashenko, Y. Bormashenko, G. Whyman, R. Pogreb, A. Musin, R. Jager, Z. Barkay, *Langmuir* **24**, 4020–4025 (2008).
34. M. Ashraf, C. Campagne, A. Perwuelz, P. Champagne, A. Leriche, C. Courtois, *J. Colloid Interface Sci.* **394**, 545–553 (2013).
35. H. Y. Erbil; C. E. Cansoy, *Langmuir* **25**, 14135–14145 (2009).
36. M.T.Z. Myint, R. Kitsomboonloha, S. Baruah, J. Dutta, *J. Colloid Interface Sci.* **354**, 810–815 (2011).
37. M. G. Krishna, M. Vinjanampati, D. D. Purkayastha, *Eur. Phys. J. Appl. Phys.* **62**, 30001 (2013).
38. Y. Gao, Y. Masuda, K. Koumoto, *Langmuir* **20**, 3188–3194 (2004).
39. K. Hashimoto, H. Irie, A. Fujishima, *Jpn. J. Appl. Physics.* **44**, 8269–8285 (2005).
40. A.V. Manole, M. Dobromir, R. Apetrei, V. Nica, D. Luca, *Cer. Intern.* **140**, 9989–9995 (2014).
41. F.K. Lee, G. Andreatta, J.-J. Benattar, *Appl. Phys. Lett.* **90**, 181928–181931 (2007).
42. Y.C. Lee, Y. P. Hong, H. Y. Lee, H. Kim, Y.J. Jung, K.H. Ko, H.S. Jung, K.S. Hong, *J. Colloid Interface Sci.* **267**, 127–131 (2003).